Corrosion of a Dense, Low-additive Si_3N_4 in High Temperature Combustion Gases

D. J. Baxter,[a]* T. Graziani,[b] H. -M. Wang[c] and R. A. McCauley[c]

[a]EC-JRC, Institute for Advanced Materials, PO Box 2, 1755 ZG Petten, The Netherlands
[b]EC-JRC-IAM, now at ISRIM, Loc. Pentima Bassa 21, Terni, Italy
[c]Center for Ceramic Research, Rutgers University, Piscataway, NJ, USA

Abstract

The oxidation/corrosion resistance of silicon nitride is determined by a number of factors, most notably the amount and chemical composition of the grain boundary phases produced as a result of adding oxides to promote densification during sintering/hot pressing. The intergranular material may be very active during high temperature exposure, producing a deleterious effect on the oxidation/corrosion processes. A method for producing silicon nitride with low levels of additives (only 0·59% Al_2O_3 and 1·22% Y_2O_3) and the benefits in terms of corrosion behaviour are described in this paper. The results of tests in combustion gases, where the concentration of sulphur in the fuel and contaminants in the ingested air have particular effects on the rate of corrosion, are reported. © 1999 Elsevier Science Limited. All rights reserved

1 Introduction

Ceramic materials maintain strength and resistance to oxidation well beyond the temperature limitations of metallic alloys. Combined with attractive physical properties, particularly low density, there is good potential for their use in systems operating at elevated temperatures. For example, more efficient combustion, with concomitant reduction in environmental emissions, can be achieved by increasing temperature, however, this would usually result in increased rates of component degradation due to corrosion. Resistance to corrosive attack is therefore one of the most important factors determining the life, and consequently the economic viability, of commercial plant. The intrinsic brittleness of ceramics and the consequent lack of confidence in mechanical reliability is gradually being overcome through compositional modification and improved production methods. Learning to design with ceramics is also progressing as more property data and more accurate degradation models are produced.

The limiting conditions for the high temperature application of silicon nitride are determined not by the inherent properties of the silicon nitride but by the properties of the whole system. The amount and composition of the intergranular phases is determined by the often complex phase equilibria at the sintering and, subsequently, the service temperature. Intergranular phase locations are not always easy to determine, but they generally are present at grain boundaries and pockets between grains. These intergranular phases either melt or soften allowing deformation under load at high temperatures. Minimizing the amount of intergranular phases at service temperatures, therefore, is one way to improve the high temperature mechanical properties.

Traditionally, sintering aid additives are introduced by mixing silicon nitride and various metal oxides by ball milling. Segregation of the sintering additives generally occurs during the mixing process of the traditional methods. Therefore, large amounts of metal oxides, over 5 to 10 wt%, are commonly used to overcome the heterogeneity of additive distribution in order to supply sufficient liquid phase to achieve full densification. During service, these metal oxides, which generally react with any silica present, may form low viscosity phases at grain boundaries and triple points that degrade the high temperature performance of the materials. One way to minimise this problem is to lower the amount of additive used. However, to obtain full densification this requires a more uniform distribution of sintering aid. Short chain-length surfactants with hydrated metalhydroxide anchor groups can act as stabilising agents as well as a surface modifying agent. This provides a

*To whom correspondence should be addressed. Fax: +31 224 263841; e-mail: baxter@jrc.nl

means of coating a powder surface in a rather uniform manner with the metal oxide that, once the hydrophillic part has been removed, can act as a sintering aid. This approach was used in this study to incorporate organic surfactants with the desired metal cations from a colloidal process as coatings on the silicon nitride particles. A low temperature, burn-out is used to convert the metal organics to oxides that then serve as liquid formers for densification. The main advantage of this type of processing is that the sintering aids are more homogeneously distributed and therefore allow full densification with less total additive.

The ability of SiC and Si_3N_4 to resist rapid degradation in corrosive environments is dependent on the formation of a slow growing surface layer in which silica is the main component. The rate of growth of this layer is closely dependent upon temperature and actual composition and morphology and so can be influenced quite strongly by participation of both sintering aids and impurities in the ceramic. While in principle, low levels of sintering aids should ensure low rates of oxidation, the effect that the particular elements have on the viscosity of the SiO_2 glass will usually be even more important. The properties and performance of the surface layer formed under purely oxidising conditions (e.g. air or O_2) will further be influenced by contaminants (most notably alkali metals such as Na) which are present in many industrial process environments.

The approach to material evaluation depends on the intended industrial application. While many different laboratory tests are used for fundamental scientific studies, few of these test methods can be carried out using test gases that accurately represent the dynamic environments found in industrial processes. Where the performance of a material is to be assessed for potential industrial application, the exposure conditions should approach as closely as possible the key aspect of the character of the industrial conditions. For these reasons, a burner rig was chosen as the main apparatus for testing the low-additive silicon nitride. Although involving many variable parameters, close control of operation of a low-velocity burner rig makes laboratory corrosion testing in complex industrially relevant environments possible.[1] This paper focuses on the corrosion behaviour of a very low additive content Si_3N_4 in dynamic, salt contaminated combustion environments produced in a low velocity burner rig. In particular, the influence of combustion gas composition is addressed. The benefits of low additive content is assessed by comparing behaviour with that exhibited by a more common Si_3N_4 composition and with sintered SiC.

2 Experimental Methods

2.1 Test materials

The test material was prepared using UBE E10 silicon nitride powder (UBE, Japan) which was milled with yttrium and aluminium 2,4 pentanedionate (Johnson Matthey, Waid Hill, MA, USA, with a composition, Y– and Al– (CH_3COCH-$COCH_3)_3$) in n-hexane in a polypropylene bottle containing silicon nitride milling media for 24 h. The amount of metal-organic compounds used was calculated to yield a nominal composition of 0.67 wt% Al_2O_3 and 1.33 wt% Y_2O_3. The analysed and calculated compositions of the UBE powder after mixing with the organic and organic burn-out are given in Tables 1 and 2, respectively. This mixture was dried at 150°C for 24 h to remove the hexane, dispersed in deionized distilled water (40 vol% solids), and pressure-cast at 0.3 MPa into bars. The bars were heated at 550°C for 4 h in air to remove the organic species before being cold isostatically pressed at 276 MPa for 5 min. Densification and sintering was carried out at 1600°C for 1 h with a nitrogen pressure of 3 bar, followed by a period of 3 h at 1875°C at 15 bar N_2. A heating rate of 600°C h^{-1} was used up to 1600°C and rate of 360°C h^{-1} was used between 1600 and 1875°C. The cooling rate was 360°C h^{-1} to 1000°C and then 600°C h^{-1} to room temperature.

TEM samples were prepared of both the as-received UBE powder and of the coated powder after organic burn-out by dipping a copper mesh into a dilute ethanol suspension and then drying under vacuum. The test pieces used for corrosion experiments were in the form of 4-point bend test bars, $3 \times 4 \times 50$ mm, with a surface roughness of 0.5μm (Ra). The materials used for comparison purposes were a sintered SiC[2] and a hot-pressed Si_3N_4[3] containing 3% Al_2O_3 and 8% Y_2O_3.

Table 1. Analysed chemical composition of the powder after mixing

Element	UBE + Y- and Al- pentanedionate (wt%)
Si	60.00
N	37.30
O	2.78
C	0.15
Al	0.31
Y	0.96

Analsis performed by Luvac Inc., Boylston, MA, USA.

Table 2. Calculated chemical composition of compounds based on the data in Table 1

Compound	wt %
SiO_2	4.21
Al_2O_3	0.59
Y_2O_3	1.22

2.2 Test conditions

For each test, bars were placed vertically on a rotating table (to ensure uniform exposure of all faces) in a low-velocity ($0.2 \, ms^{-1}$) burner rig. The tests were carried out at temperatures of 1100, 1200 and 1300°C each for a total time of 50 h, divided in eight equal cycles of 6·25 h. After each thermal cycle the bars were cooled freely in laboratory air and weighed. The corrosion environment was produced by burning either a 1 wt% sulphur marine diesel fuel or a 0·01 wt% sulphur kerosene (Jet A1) in air contaminated with artificial ocean water. The ocean water was made to the standard ASTM D1141 (containing the following proportions of salts; 59% NaCl, 10% Na_2SO_4, 26% $MgCl_2.6H_2O$, 3% $CaCl_2$ and 1·7% KCl). The ratio of air to fuel was 28:1 (by weight) and resulted in a nominal input of 310 or 31 ppm of SO_2, for 1 and 0·01% sulphur fuel, respectively. The total flux of sea salt injected into the burner rig was 13 mg cm^{-2} h^{-1}, which is equivalent to 4 mg cm^{-2} h^{-1} of Na. Calculations of the combustion gas compositions using the Solgasmix computer program[4] (assuming thermodynamic equilibrium) showed that no condensed phases should be produced in either of the two combustion gases at all temperatures of test. The simultaneous exposure of pure alumina (considered inert) test pieces confirmed that no condensation occurred during the tests. The partial pressures of the main combustion products are listed in Table 3. Tests were also conducted in dry air (less than 5 ppm H_2O) for comparison purposes. Flexural strength tests (4 point) were carried out according to the standard EN843-1, using an outer span of 40 mm and an inner span of 20 mm.

3 Results

3.1 Properties of the fabricated test material

TEM examination of the uncoated UBE powder (Fig. 1) showed that the silicon nitride had a clean surface with a thin amorphous layer of approximately 2–3 nm thickness. Energy dispersive analysis revealed that only Si, N, and O were present. In contrast, the coated powder exhibited a much rougher surface (Fig. 2). The surface bumps were

on the order of 5–6 nm in diameter and when analysed by EDS were found to contain Al and Y. The final density after sintering was 3·16 g cm^{-3}, with closed porosity of less than 1%. Some of the measured properties of the dense sintered material are given in Table 4.

3.2 Corrosion test results

Corrosion tests in the burner rig produced the weight changes shown in Fig. 3(a). In the combustion gas of the 1 wt% sulphur fuel, the amount of weight gained increased with increasing temperature and the rate was approximately parabolic, except at 1300°C where a slight acceleration
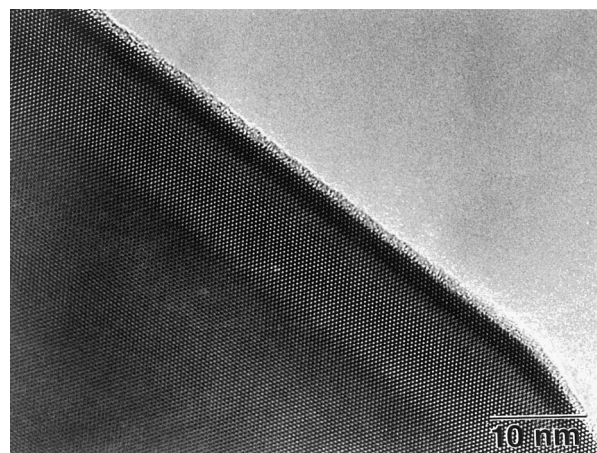

Fig. 1. TEM image of the clean surface of an uncoated UBE silicon nitride powder particle.
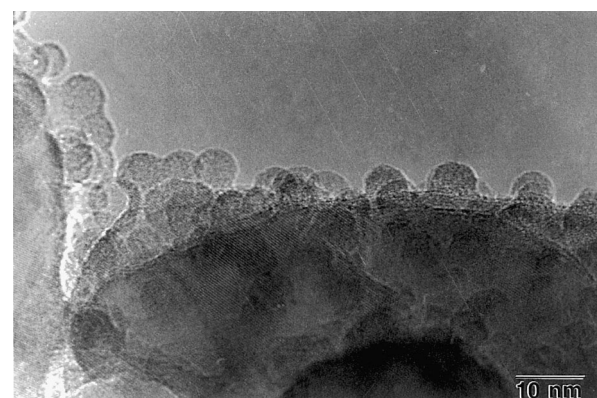

Fig. 2. TEM image of silicon nitride particles after coating with sintering additives.

Table 3. Partial pressures (Pa) of the main species in the combustion gases (total pressure: 10^5 Pa)

Temperature (°C)	Fuel	pSO₂	pSO₃	PNaOH	pNa₂O	pNa₂SO₄
1100	0·01%S	1.6×10^{-1}	8.8×10^{-3}	3.5×10^{-1}	1.3×10^{-9}	1.2×10^{-2}
1200	0·01%S	2.7×10^{-1}	5.3×10^{-3}	5.5×10^{-1}	5.8×10^{-9}	1.0×10^{-3}
1300	0·01%S	2.8×10^{-1}	3.2×10^{-3}	7.9×10^{-1}	2.1×10^{-8}	1.1×10^{-4}
1100	1·0%S	3.0×10	1.0×10^{0}	1.6×10^{-1}	2.8×10^{-10}	3.0×10^{-1}
1200	1·0%S	3.0×10	5.8×10^{-1}	4.7×10^{-1}	4.3×10^{-9}	8.3×10^{-2}
1300	1·0%S	3.1×10	3.6×10^{-1}	7.7×10^{-1}	2.0×10^{-8}	1.1×10^{-2}

Table 4. Selected physical and mechanical properties

Phase analysis	$100\%\beta-Si_3N_4$(by XRD)
Density (Archimedes)	$3.160 \pm 0.002 \times 10^4 g\,m^{-3}$
Vickers hardness	14.1 ± 0.2 GPa
Fracture toughness (indentation method)	5.90 ± 0.15 at 49 N to 6.48 ± 0.19 MPa m$^{-1/2}$ at 294 N
Mean MOR (4-point)	750 ± 29 MPa at room temperature
	625 MPa in air at 1200°C
	562 MPa in air at 1300°C
Weibull modulus (36 test pieces)	10
Creep rate	3×10^{-7} s^{-1} at 100 MPa in air at 1400°C

occurred after 37 h of exposure. (For comparison purposes, the weights gained by a higher-additive content Si_3N_4 and sintered SiC in the same combustion gas are shown in Fig. 4). After 50 h the corrosion products were an amorphous silicate glass, containing Na (additionally Al at 1300°C) and located mainly in the outer region of the scale, and cristobalite (essentially pure SiO_2), constituting an inner layer adjacent to the ceramic surface. The amount of cristobalite increased with increasing temperature. The total scale thickness ranged from 1–2 μm at 1100°C, to 3–5 μm at 1200°C, to 7–10 μm at 1300°C. An example of a cross section

through the surface scale formed at 1300°C is shown in Fig. 5. Compared with oxidation in air, where the surface scale was also composed of an inner cristobalite layer and an outer amorphous glass, the rate of scale formation was very similar [compare the data in Figs 3(a) and 6].

Exposure to the 0.01 wt% sulphur fuel combustion gas gave the weight gains shown in Fig. 3(b).
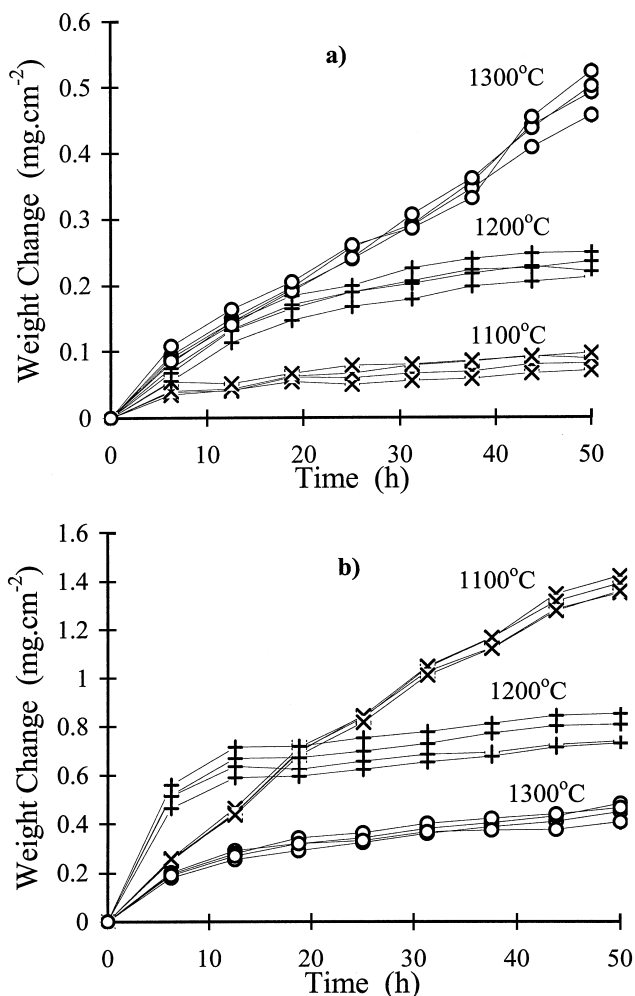

Fig. 4. Weight change data for SiC (after Graziani *et al.*[2]) and Si_3N_4 + 3% Al_2O_3 + 8% Y_2O_3 (after Graziani *et al.*[3]) in a 1 wt% sulphur fuel combustion gas in a low velocity burner rig.

Fig. 3. Weight change data after exposure in combustion gases in the burner rig: (a) 1 wt% sulphur; (b) 0.01 wt% sulphur fuel combustion gases.
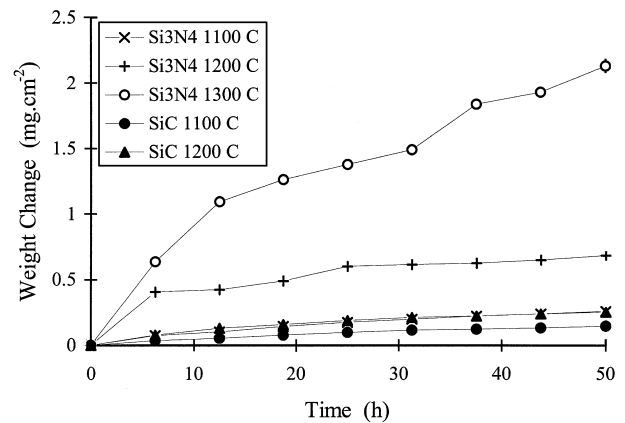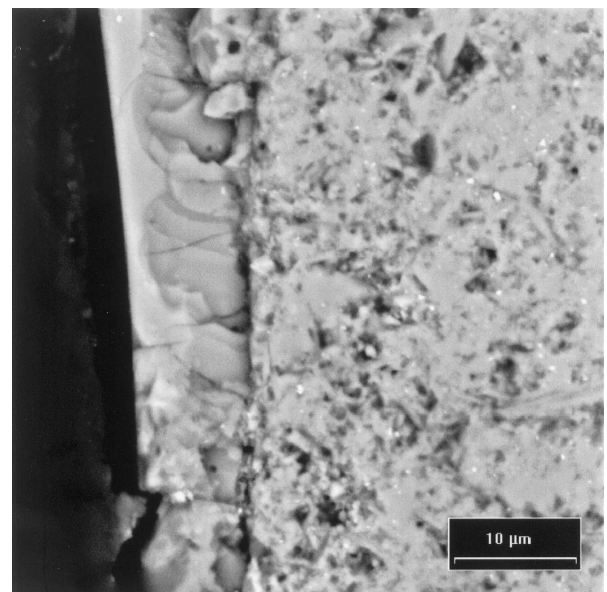

Fig. 5. SEM micrograph of a cross-section through a test piece after exposure to the 1 wt% sulphur fuel combustion gas at 1300°C for 50 h.
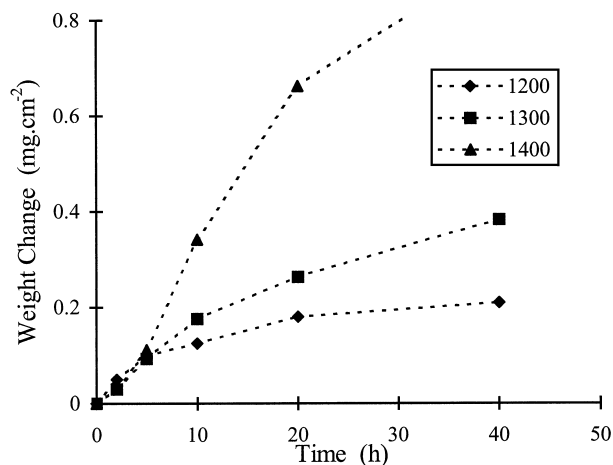
Fig. 6. Weight change data for the low-additive Si₃N₄ in air.

In these tests the trend of weight gain as a function of temperature was reversed (cf. 1 wt% S fuel). At 1100°C, the scale was of non-uniform thickness ranging from 20 to 60 μm (Fig. 7, top), and contained a large volume fraction of both cristobalite and tridymite crystals (though not forming a continuous layer) in an amorphous Na-containing silicate. Large pores were distributed throughout the scale thickness. Yttrium was depleted to a depth of about 10 μm immediately beneath the ceramic surface. A similar scale morphology was produced at 1200°C (Fig. 7, centre), except that the crystalline material had a more compact appearance, constituting an almost continuous layer in the scale that ranged in thickness from 15 to 40 μm. At 1300°C, most of the scale was relatively thin (8–10 μm), containing a continuous inner layer of cristobalite (no tridymite) with a covering of Na-containing silicate (Fig. 7, bottom). However, also present were a few large 'eruptions' in the scale up to a total thickness of 120 μm (70 μm beneath the original ceramic surface and 50 μm above) (Fig. 8). This form of locally accelerated attack was hardly evident in the weight change data [Fig. 3(b)], highlighting a potentially weakness in using weight data as a method of monitoring the progress of corrosion. The appearance of the eruptions was noticed during low magnification optical examination of test pieces surfaces only before the final thermal cycle. Further examination in the SEM failed to reveal the reason for breakdown of the normally protective surface layer at particular locations. It is noted, however, that cristobalite was the major phase in the corrosion product formed in the pits and that β-Si₃N₄ grains had become incorporated in the SiO₂ (Fig. 8). It is possible therefore that accelerated attack of the ceramic involved mainly reaction with the intergranular phase. Whilst the tendency for pitting/roughening of the ceramic appeared greater after exposure to the low-sulphur fuel, the resultant reduction (40%) in room
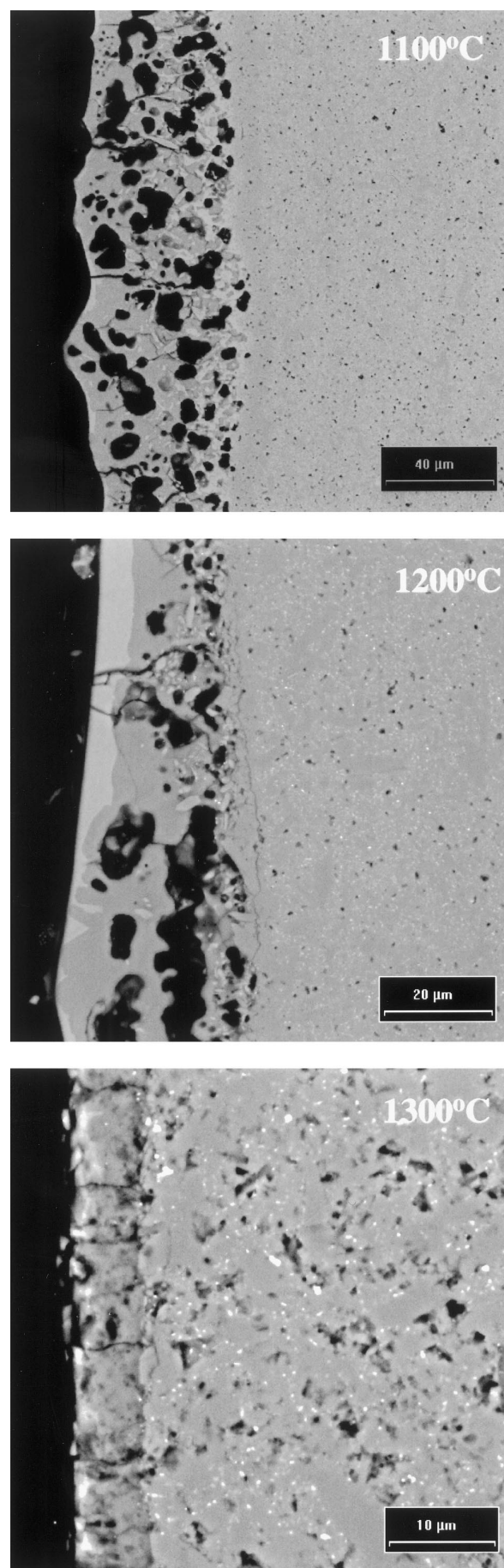

Fig. 7. SEM micrographs of cross-sections through test pieces after 50 h exposure to the 0·01 wt% sulphur combustion gas at 1100°C (top), 1200°C (centre) and 1300°C (bottom).

Fig. 9. Results of 4-point flexural strength tests carried out at room temperature (four test pieces per test condition).
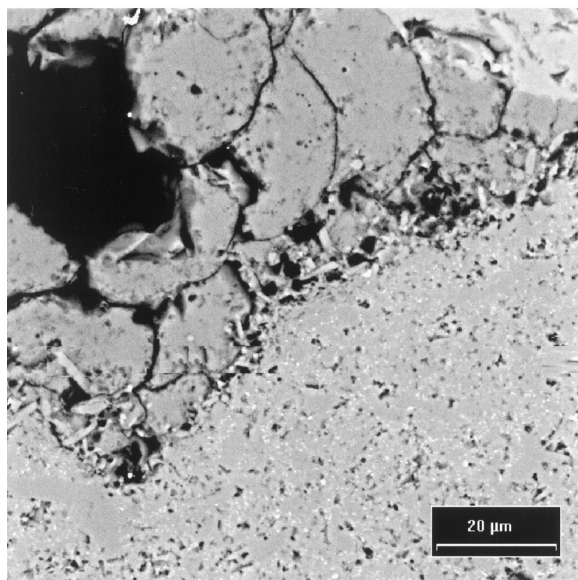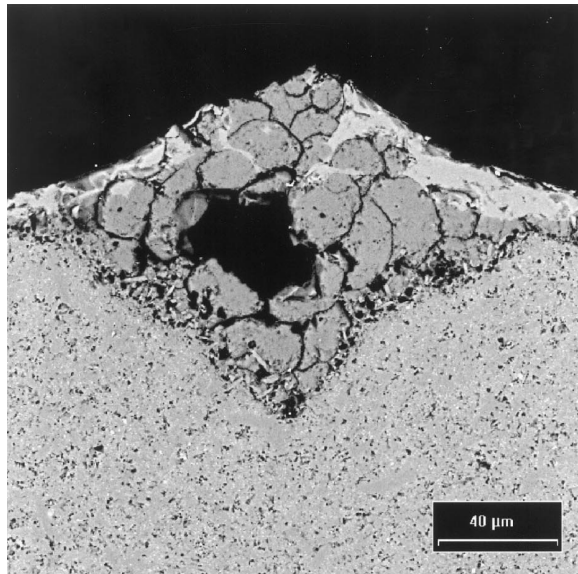

Fig. 8. SEM micrographs of cross-sections through a test piece showing severe localised pitting after 50 h exposure to the 0·01 wt% sulphur fuel combustion gas at 1300°C.

temperature flexural strength was largely independent of test conditions (Fig. 9).

4 Discussion

4.1 Powder processing

Incorporation of the sintering aids in a uniform manner in a densified ceramic requires control over the distribution of phases during fabrication. Conventional processing by ball milling will not provide this; there will be fluctuations in the amount of the additive over the green and final microstructures depending upon the milling time, milling media, impurity level, and powder particle size and surface condition. An alternative to conventional ball milling is the coating of the silicon nitride with the desired sintering aids added as a metal complex.
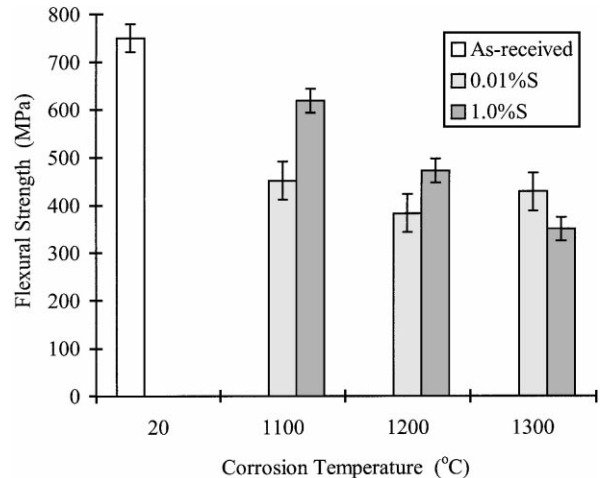
The surface coatings appeared non-crystalline and did not fully cover the surface. The non-continuous nature of the coating can be explained by the fact that only certain surface sites (silanol groups) reacted with the metal-organics via chemical adsorption. The coatings modified the surface of the silicon nitride to act like yttria or alumina as evidenced by a shift in the isoelectric point from pH = 6·0 for the as-received UBE powder to about pH = 8·5 for the coated powder. The isoelectric points of alumina and yttria are at about pH = 9·0

4.2 Corrosion behaviour

From the results obtained in this study, three particular points of interest arise; first, the corrosion behaviour in a combustion gas compared to that in air; second, the effect of combustion gas composition; and third, the behaviour of low-additive Si_3N_4 compared to that of other Si_3N_4 and SiC.

Oxidation tests in air are often carried out as a first step in the assessment of the environmental resistance of a material to be used in high temperature applications. In some instances, the results of a simple air test can provide a good guide to the stability of a material in what may be considered a simple 'oxidising' atmosphere containing the minimum of contaminants/impurities. Both of the combustion environments used in this work were created by burning liquid fuels under air-excess conditions with the result that the oxygen partial pressure was only slightly less than that of air. The rate of material degradation, as measured by change in weight, was very similar for the corresponding air and 1 wt% sulphur fuel tests. In both environments the rate of scale formation was approximately parabolic, suggesting that diffusion was the rate controlling process, with the additional presence of Na in the burner rig tested specimens apparently having a negligible effect on the

rate. So what happened when the material was exposed to the 0·01 wt% sulphur fuel environment? Higher weight gains were observed and increasing temperature reduced the rate of degradation. The main difference was the amount of Na incorporated into the growing silicate scale. The activity of Na (most importantly Na_2O) in combustion environments should be controlled by the concentration of sulphur in the combustion gas, in the form of SO_3.[5] A high pSO_3 sets a low Na activity and vice versa according to the equation:

$$Na_2SO_4 = Na_2O + SO_3 \qquad (1)$$
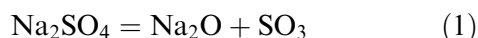
Assuming the main degradation reaction for SiO_2 to involve Na_2O,

$$2SiO_2 + Na_2O = Na_2Si_2O_5 \qquad (2)$$

whether accelerated corrosion takes place should depend upon the sulphur content of the fuel combusted. Hence, a low pSO_3 ('basic' combustion gas atmosphere) should be associated with high Na uptake by (acidic) SiO_2-forming ceramics. The formation of low viscosity Na-silicates results in high rates of corrosion compared with when pure SiO_2 is formed as a surface oxidation product. Calculated equilibrium partial pressures for the main Na-containing species show that the pSO_3 affects the pNa_2SO_4 over the whole range of test temperatures and affects the pNa_2O only at 1100°C. The partial pressure of NaOH is independent of pSO_3 over the whole test temperature range. The equilibrium calculations, made using thermodynamic data for pure substances at unit activity, indicate that no condensed species should be formed. The thermodynamic data thus suggest that as at lower temperatures when condensed species are present, Na_2O should also be the key species promoting accelerated attack at temperatures above the dew point of condensable species.

The next question concerns the reason for the rate of reaction decreasing with increased temperature. The fact that devitrification of SiO_2 is favoured by increased temperature and by the presence of metal ions[6] explains why more crystalline material was formed on the ceramic when exposed to the 0·01 wt% sulphur fuel combustion gas environment. Since the rate of transport through crystalline SiO_2 should be lower than that through the amorphous silica/silicate,[7] an increased presence of crystalline SiO_2 should be accompanied by lower rates of scale growth, provided that the crystalline layer is continuous. Therefore, the morphology of the surface layer, particularly with respect to the crystalline phase(s), would likely have a major influence on corrosion rate, leading

to the observed temperature inversion effect. The mechanism involved in the severe form of pitting attack at 1300°C has not been identified. While it appeared that accelerated attack of the sintering additives takes place within the pits, it is possible that initiation of the pitting process could have been due to damage incurred in the SiO_2-rich surface layer (e.g. due to for example cracking of the cristobalite during thermal cycles). Pitting attack did not, however, have any additional deleterious effect on room temperature flexural strength.

Sintering additives are involved in the oxidation of dense Si_3N_4 ceramics. Aluminium enters SiO_2 by substitution (Al^{3+} for Si^{4+}) thereby increasing ionic conductivity and decreasing molecular oxygen transport,[7] whereas Y usually forms discrete disilicate ($Y_2Si_2O_7$) crystals which contribute to extra oxygen uptake without conferring additional oxidation protection. Reducing the additive content from 11 to 2 total wt% decreases the amount of weight gained to the extent that with only 0·59% Al_2O_3 and 1·22% Y_2O_3 the rate of scale growth approaches that on sintered SiC [seen by comparing Figs 3(a) and 4]. This is clearly a positive result, but it does not clarify the individual roles of Al and Y. Ideally, from the results of this work, the intention should be to select material composition, properties and microstructure to promote the formation of a continuous crystalline SiO_2 surface layer during high temperature exposure. Caution should, however, be exercised owing to possible mechanical instabilities that could result from phase transformations and mismatches in thermal properties leading to cracking of the crystalline component of the surface layer. Cracks in amorphous scales appear to heal rapidly upon re-exposure to high temperatures compared to cracks in crystalline material. Some loss of protection to the ceramic may thus occur with the latter. It also has to be stated that a simple oxidation test in air cannot be used as a substitute for a corrosion test in a low-sulphur fuel combustion environment.

5 Conclusions

Sintering additives play an important role in the oxidation/corrosion behaviour of Si_3N_4, reducing the total additive content reduces the rate of reaction. A method for the preparation of Si_3N_4 with very low sintering additive content, via a process of coating of individual powder particles, has been demonstrated. This method was successful in obtaining dense materials at a modest sintering temperature. The resultant rate of oxidation in dry air was similar to that of sintered SiC. In combustion environments, the rate of corrosion is

dependent upon pSO$_3$, and thus on fuel sulphur content. The corrosion rate with a high pSO$_3$ is similar to that of oxidation in air, whereas with a low pSO$_3$ a high rate of corrosion is observed. A low pSO$_3$ permits basic attack of the acidic SiO$_2$ and the rapid incorporation of Na into the SiO$_2$-rich surface scale. In the future, it is recommended that materials be selected, preferably with low amounts of sintering additives, that promote the formation of a silica-rich surface layers that contain crystalline silica as a major component. A balance, however, must be maintained between the amounts of amorphous and crystalline components in order that the propensity for cracking of the crystalline material does not lead to seriously enhanced attack particularly under thermal cycling conditions.

Acknowledgements

References

1. Nicholls, J. R. and Saunders, S. R. J., Comparison of hot-salt corrosion behaviour of superalloys in high and low velocity burenr rigs. *High Temp. Tech.*, 1987, **7**, 193–201.
2. Graziani, T., Baxter, D. and Nannetti, C. A., Degradation of SiC-based materials in a high temperature combustion environment. *Key Engineering Materials*, 1996, **113**, 153–164.
3. Graziani, T., Baxter, D. and Bellosi, A., Corrosive degradation of a dense Si$_3$N$_4$ in a burner rig. *J. Mat. Sci.*, 1997, **32**, 1631–1637.
4. Eriksson, G., Thermodynamic studies of high temperature equilibria: VII. SOLGASMIX, a computer program for calculation of equilibrium compositions in multiphase systems. *Chemica Scripta*, 1975, 8, 100–103.
5. Jacobson, N. S, Sodium Sulphate: Deposition and Dissolution of Silica. *Oxid. Met.*, 1989, **31**, 91–103.
6. Singhal, S. C., Thermodynamics and kinetics of oxidation of hot-pressed silicon nitride. *J. Mat. Sci.*, 1976, **11**, 500–509.
7. Lamkin, M. A., Riley, F. L. and Fordham, R. J., Oxygen mobility in silicon dioxide and silicate glasses: a review. *J. Eur. Ceram. Soc.*, 1992, **10**, 347–367 .